Mem. S.A.It. Vol. 85, 227

Memorie della

Detailed element abundances of SkyMapper EMP stars: first results of the high-resolution spectroscopic follow up

Heather R. Jacobson[1], Martin Asplund[2], Michael S. Bessell[2], Andrew R. Casey[2], Gary S. Da Costa[2], Anna Frebel[1], Stefan C. Keller[2], Karin Lind[3], John E. Norris[2], Brian P. Schmidt[2], Patrick Tisserand[2], and David Yong[2]

[1] Massachusetts Institute of Technology – Kavli Institute of Astophysics and Space Research, 77 Massachusetts Avenue, Cambridge, MA, 02139, USA
e-mail: hrj@mit.edu

[2] Research School of Astronomy and Astrophysics, Australian National University, Mount Stromlo Observatory, Cotter Road, Weston, ACT 2611, Australia

[3] Institute of Astronomy, University of Cambridge, Madingley Road, Cambridge CB3 0HA, United Kingdom

Abstract. The multi band photometry of SkyMapper's Southern Sky Survey is designed to search for extremely metal-poor (EMP) stars. The best candidates have been observed with low-resolution spectroscopy to confirm their low metallicities, and then with high-resolution spectroscopy to determine their detailed element abundances. So far, high-resolution Magellan/MIKE spectra have been obtained for over 200 EMP candidates. Here we present the results for the first ~14 months of this new effort, during which time the photometric candidate selection has been continuously improved. Of the 50 most recently observed EMP candidates, roughly half have [Fe/H] ≤ -3, with 3 stars having [Fe/H] ≤ -3.5. Our analysis shows these metal-poor stars to have typical halo star abundance patterns. These results clearly demonstrate SkyMapper's capability to find large numbers of EMP stars which will vastly improve our understanding of the earliest star formation processes and the onset of chemical evolution.

Key words. Stars: abundances – Stars: atmospheres – Stars: Population II – Galaxy: globular clusters – Galaxy: abundances – Cosmology: observations

1. Introduction

The chemical enrichment history of the universe is recorded in the element abundance patterns of stars formed at different epochs in its formation and evolution. The most metal-poor stars (those with [Fe/H] < -3) formed out of gas that was enriched by at most only a handful of individual enrichment events, most likely the supernova explosions of massive stars (e.g., Norris et al. 2013). Though these extremely metal-poor (EMP) stars comprise a very small fraction of the stellar population in the Milky Way halo, they are nonetheless very valuable, since their abundance patterns can be used to constrain the mass range of Population III stars, the nature of their supernova explosions, and the element yields of those supernovae.

The last few decades have seen large dedicated surveys searching for these EMP stars, mainly through the strength (or rather, relative weakness) of strong spectral features like the Ca II K line as indicators of overall stellar metallicity (Beers et al. 1992; Christlieb et al. 2008; Frebel et al. 2006). The SkyMapper Southern Sky Survey represents the latest generation of this type of survey: it utilizes the relative efficiency of photometric surveys to scan the entire southern sky, but mimics previous spectroscopic surveys' focus on the Ca II K line (Keller et al. 2007). It does this by adding a narrow-band filter centered on the Ca II K line to the standard SDSS-like *ugriz* filter system (Bessell et al. 2011).

The addition of this metallicity-sensitive filter allows for different color combinations that constrain stellar temperature, surface gravity and metallicity based on photometry alone, allowing for the identification of candidate EMP stars. Such photometrically-selected candidates are then followed up with low-resolution spectroscopy to get a direct measure of line strengths; the most promising EMP candidates confirmed by low-resolution spectra are then passed on for high-resolution spectroscopic follow-up to determine element abundances from individual absorption lines (Keller et al., in prep.). This work presents the analysis of the high-resolution data of SkyMapper EMP candidates obtained over the first ∼14 months of follow-up observations.

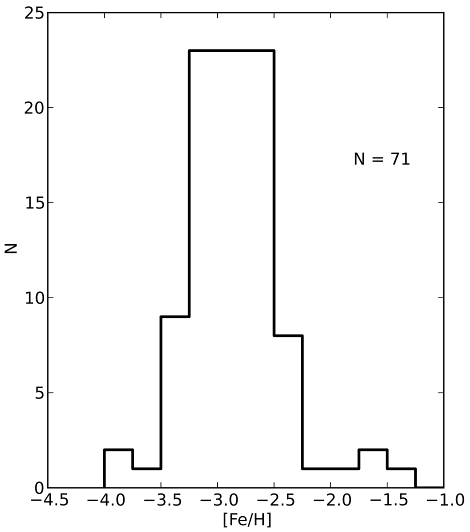

Fig. 1. The range of [Fe/H] values determined for this sample of SkyMapper EMP candidates. Note that the metal-rich end is incomplete due to the exclusion of many stars with [Fe/H] $>$ −2.2. The mean [Fe/H] of the sample is −2.80. The bin size is 0.25 dex.

2. Spectroscopic sample

Our high-resolution spectroscopic sample was obtained with the MIKE spectrograph on the Magellan-II Clay telescope (Bernstein et al. 2003). Observations were made using the 0.7" or 1.0" slit, depending on seeing conditions, resulting in resolving powers R = 35,000 (28,000) and 28,000 (22,000) in the blue and red for the 0.7 (1.0) slits, respectively. Our observations can be considered as "snapshot" spectra, with exposure times ranging from 5 minutes to two hours per star. The spectra have median signal-to-noise ratios of 31 and 47 per pixel in the blue and red, respectively.

The first few high-resolution observing campaigns were done as the photometric selection technique was continually being refined; as a result, many observed stars turned out to be relatively metal-rich. Consequently, for this analysis, we have taken only the ∼20 most metal-poor stars from these early campaigns, making a metallicity cut at [Fe/H] $\leq$ −2.2. This set of stars, combined with those observed in two later observing runs, comprise the sample considered here of 71 EMP candidates.

3. Analysis

Stellar atmospheric parameters for this sample were obtained using the "classical" spectroscopic technique, based on equivalent width measurements of Fe I and Fe II lines. We followed the methods described in Frebel et al. (2013), to which we refer the reader for de-

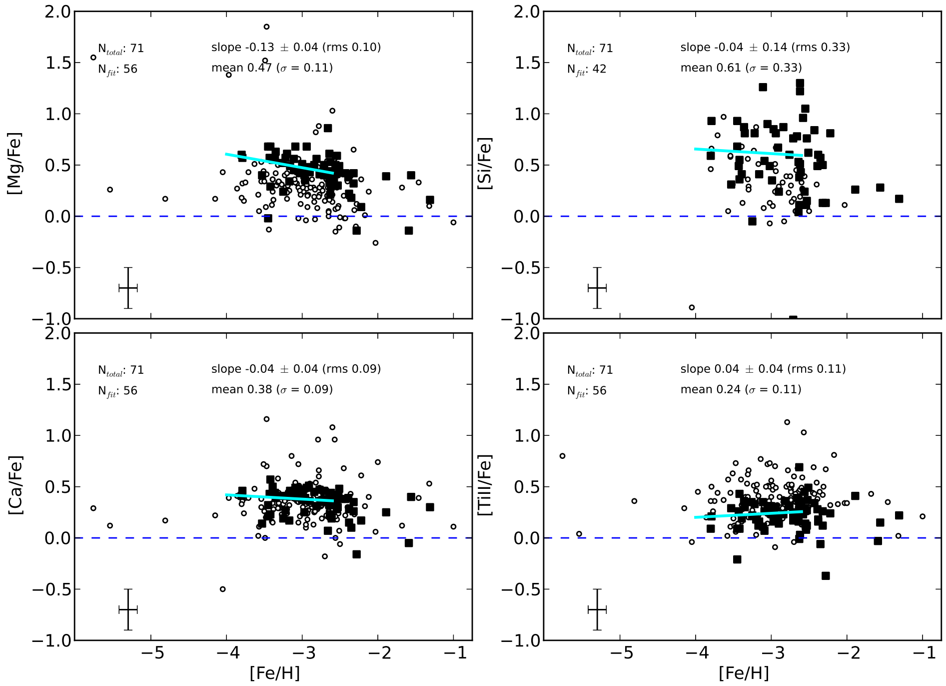

Fig. 2. The [X/Fe] versus [Fe/H] of this sample for Mg, Si, Ca and Ti (filled squares), along with those of Yong et al. (2013, open circles). The cyan line is the line of best fit based on a regression analysis of all stars in our sample with [Fe/H] ≤ -2.5, the parameters of which are also indicated in each panel. See text for details.

tails. This method applies a correction to the spectroscopic temperatures which places them roughly on the same scale as those determined via photometry. Surface gravities, microturbulent velocities and [M/H] values were then updated as necessary. Element abundances were then determined using the above atmospheric parameters, and either equivalent width measurements or spectrum synthesis of absorption features.

4. Results

4.1. Metallicity distribution function

Fig. 1 shows the distribution of [Fe/H] values for our stellar sample. There is a broad peak around [Fe/H] = -2.8, but we remind the reader that the distribution above [Fe/H] = -2.2 is incomplete due to the exclusion of many stars more metal-rich than that value. Of the 71 stars, 25 have [Fe/H] ≤ -3.0, three of which have [Fe/H] < -3.5. It is worth noting that the majority of the stars below [Fe/H] < -3 were observed in the last two observing runs, evidence of the great improvement in the photometric candidate selection over time.

4.2. Element abundance patterns

The [X/Fe] ratios versus [Fe/H] for the α elements Mg, Si, Ca and Ti are shown in Fig. 2. Our sample (filled squares) is plotted with the large homogeneous sample of Yong et al. (2013, open circles) as a comparison sample. Following that work, to investigate the behavior of [X/Fe] with [Fe/H], we performed a linear regression analysis on each abundance distribution for stars with [Fe/H] ≤ -2.5. Stars with [X/Fe] ratios more than 2σ away from the line of best fit were removed and the linear

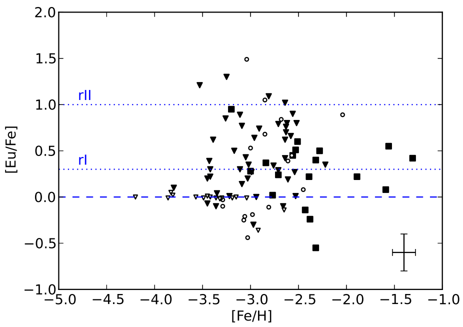

Fig. 3. [Eu/Fe] versus [Fe/H] for the SkyMapper sample (filled symbols), along with those from François et al. (2007). Upper limits are denoted by triangles, and the ranges of [Eu/Fe] exhibited by r-I and r-II stars are shown with dotted lines.

regression performed again. The resulting line of best fit is shown as the cyan line, with the slope, its error, the rms scatter about the line of best fit, as well as the mean [X/Fe] ratio and its standard deviation shown in each panel. The number of stars used in the fit is also given.

The slopes are consistent with zero for all elements except Mg, and the scatter about the mean [X/Fe] ratio is ~0.1 dex, consistent with that seen in other studies of EMP stars (Cayrel et al. 2004; Yong et al. 2013). The scatter for Si is larger, but this is more likely due to the difficulty in measuring the few weak Si lines available in these spectra. Figure 2 demonstrates that the SkyMapper EMP stars are indeed typical EMP stars found in the halo. The abundance patterns of the other elements analyzed in this study (Fe-peak and neutron capture elements) also have similar distributions to those of other EMP star studies in the literature. Interestingly, however, this sample does not contain any carbon enhanced stars, the relative fraction of which is known to increase with decreasing [Fe/H] (e.g., Yong et al. 2013).

4.3. R-process enhanced stars

EMP stars with measurable Eu absorption features in their spectra are categorized as r-process enhanced stars: those with $[Eu/Fe] \geq 1.0$ are so-called r-II stars, while those with $0.3 \leq [Eu/Fe] < 1.0$ are r-I stars (Barklem et al. 2005). Fig. 3 shows the Eu abundances of the SkyMapper stars versus [Fe/H]. For most stars, only an upper limit on the Eu abundance could be obtained (shown as triangles), but some stars had measurable Eu lines. Indeed, one star has [Eu/Fe]~1, and 8 are r-I stars.

5. Conclusions

The element abundance analysis of the first high-resolution spectroscopic followup of EMP star candidates identified in the SkyMapper Southern Sky Survey has confirmed their EMP status. Roughly one-third of the sample have $[Fe/H] \leq -3$ and element abundance patterns typical of other halo stars at similar metallicities. This successfully demonstrates SkyMapper's ability to identify EMP stars via photometry. SkyMapper's survey of the entire southern sky promises to greatly increase the number of stars confirmed to have $[Fe/H] < -3$, the element abundances of which will help answer many scientific questions regarding the nature of Pop III stars and the formation and evolution of galaxies.

Acknowledgements. AF is supported by NSF Career Grant AST-6927611. MSB, GDaC and SK are supported in part by Australian Research Council Discovery Projects grant DP120101237.

References

Barklem, P. S., Christlieb, N., Beers, T. C., et al. 2005, A&A, 439, 129
Beers, T. C., Preston, G. W., & Shectman, S. A. 1992, AJ, 103, 1987
Bernstein, R., Shectman, S. A., Gunnels, S. M. et al. 2003, Proc. SPIE, 4841, 1694
Bessell, M., Bloxham, G., Schmidt, B., et al. 2011, PASP, 123, 789
Cayrel, R., et al. 2004, A&A, 416, 1117
Christlieb, N., Schörck, T., Frebel, A., et al. 2008, A&A, 484, 721
François, P., et al. 2007, A&A, 476, 935
Frebel, A., Christlieb, N., Norris, J. E., et al. 2006, ApJ, 652, 1585
Frebel, A., et al. 2013, ApJ, 769, 57

Keller, S. C., Schmidt, B. P., Bessell, M. S., et al. 2007, PASA, 24, 1
Norris, J. E., Bessell, M. S., Yong, D., et al. 2013, ApJ, 762, 25
Yong, D., Norris, J. E., Bessell, M. S., et al. 2013, ApJ, 762, 26